HAL: HARMONIC LEARNING IN HIGH-DIMENSIONAL MDPS

Anonymous authors
Paper under double-blind review

ABSTRACT

Since the initial successes of deep reinforcement learning on learning policies purely by interacting with complex high-dimensional state representations and a decade of extensive research, deep neural policies have been applied to a striking variety of fields ranging from pharmaceuticals to foundation models. Yet, one of the strongest assumptions of reinforcement learning is to expect to receive a reward signal from the MDP. While this assumption comes in handy in certain fields, i.e. automated financial markets, it does not naturally fit in many others where the computational complexity of providing such a signal for the task at hand is larger than in fact learning one. Thus, in this paper we focus on learning policies in MDPs without this assumption, and study sequential decision making without having access to information on rewards provided by the MDP. We introduce harmonic learning, a training method in high-dimensional MDPs, and provide a theoretically well-founded algorithm that significantly improves the sample complexity of deep neural policies. The theoretical and empirical analysis reported in our paper demonstrates that harmonic learning achieves substantial improvements in sample efficient training while constructing more stable and resilient policies that can generalize to uncertain environments.

1 INTRODUCTION

The capabilities and skills obtained via interacting with a given environment solely based on observations and receiving rewards upon taking actions in high-dimensional state observation MDPs gained substantial acceleration with the recent advancements in deep reinforcement learning research (Mnih et al., 2016; Kapturowski et al., 2023; Abel et al., 2023; Flennerhag et al., 2023). Currently, from automated financial markets to solving complex games (Schrittwieser et al., 2020) to designing algorithms (Fawzi et al., 2022; Mankowitz et al., 2023), several different fields from pharmaceuticals (Popova et al., 2018; Korshunova et al., 2022) to self-operating vehicles and large language models (Touvron et al., 2023) benefited from the advancements achieved in deep sequential decision making algorithms that can learn functioning policies in high-dimensional observation MDPs. Yet, there is still a concrete assumption in reinforcement learning that we do have access to the reward function of the MDP. From bee foraging to human decision making the reward signal for natural intelligence is complicated and a non-stationary function of manifold inputs (Doya & Sejnowski, 1994; Montague et al., 1995; Schmajuk & Zanutto, 1997). Thus, towards targeting capabilities and skills that natural intelligence can currently achieve we do have to consider and study the reward functions formed over the centuries of evolution.

Analyzing the amount of experiences one has to obtain to function in a given environment is one of the foundational questions that has been studied so far (Kearns & Singh, 1999; Kakade, 2003). Recent studies argued that policies trained in the absence of a reward signal can in fact learn faster. Orthogonal to these advances while the instabilities of deep neural networks under non-robust directions has been discussed (Goodfellow et al., 2015), recent work also demonstrated that these instabilities are currently also present in deep neural policies (Huang et al., 2017). Furthermore, even more recent studies demonstrated that these non-robust directions can be semantically meaningful changes to the environment (Korkmaz, 2024). Thus, in this paper we focus on the sample-efficiency and robustness of the policies that can learn functioning strategies without the reward signal provided by the MDP and ask the following questions:

- *How can we build agents that can learn neural policies with fewer interactions?*
- *What are the foundational building blocks towards constructing policies that can make resilient and robust decisions in unstable and non-robust environments?*
- *How can we analyze and quantify the robustness of deep sequential decision making policies with high-dimensional state observations spectrally?*

Hence, to answer these questions in this paper we focus on analyzing the spectral properties of deep inverse reinforcement learning, and make the following contributions:

- We introduce a theoretically well-founded algorithm called harmonic learning that improves the sample complexity of deep sequential decision making algorithms, and learns policies that are more stable and robust. We conduct experiments in the Arcade Learning Environment (ALE) with high dimensional state observation MDPs, and the experimental results reported in our paper demonstrate that our harmonic learning algorithm, i.e. HAL, achieves substantial sample-efficiency resulting in requiring up to $20\times$ fewer samples while achieving better performance.
- We propose a theoretically justified novel method to analyze deep neural policy robustness in the frequency spectrum. We compare the vulnerabilities and volatilities of the state-of-the-art imitation learning policy to the vanilla deep reinforcement learning policy in high dimensional state representation MDPs. Our method reveals the spectral contrast between the vanilla deep reinforcement learning policies and the state-of-the-art deep sequential decision making policies that can learn without a reward function.
- Furthermore, we analyze the generalization capabilities, natural robustness and overfitting of the state-action value function. Our analysis further demonstrates that harmonic learning leads to policies that are substantially more robust and generalizable.

2 Background and Preliminaries

2.1 Preliminaries

A Markov Decision Process (MDP) is represented as a tuple $\langle \mathcal{S}, \mathcal{A}, \mathcal{P}, r, \gamma, \tau_0 \rangle$ of a set of states $\mathcal{S}$, a set of actions $\mathcal{A}$, transition probability distribution $\mathcal{P}(s_{t+1}|s_t, a_t)$, and a reward function $r : \mathcal{S} \times \mathcal{A} \to \mathbb{R}$, discount factor γ, and initial state distribution τ_0. The objective in reinforcement learning is to learn a policy that will maximize the expected discounted cumulative rewards obtained by the policy $\pi : \mathcal{S} \to \mathcal{P}(\mathcal{A})$. This objective can be achieved via $\mathcal{Q}$-learning that essentially learns a $\mathcal{Q}$ function $\mathcal{Q} : \mathcal{S} \times \mathcal{A} \to \mathbb{R}$ that will assign values to each state-action (s, a) pair to reveal what would be the expected cumulative discounted rewards obtained if the action a is taken in state s. The $\mathcal{Q}$-function is learnt via iterative Bellman update $\mathcal{Q}(s_t, a_t) = r(s_t, a_t, s_{t+1}) + \gamma \sum_{s_t} \mathcal{P}(s_{t+1}|s_t, a_t) \max_a \mathcal{Q}(s_{t+1}, a)$ (Watkins, 1989). The value function is defined to be $\mathcal{V}(s) = \max_a \mathcal{Q}(s, a)$. Upon the construction of the state-action value function the policy executes the action that maximizes the state-action value function $\hat{a} = \arg\max_{a \in A} \mathcal{Q}(s, a)$. In settings where the state or action space have high-dimensional representations the state-action value function is approximated via a deep neural network.

$$\theta_{t+1} = \theta_t + \alpha(r(s_t, a_t, s_{t+1}) + \gamma \max_a \mathcal{Q}(s_{t+1}, a; \theta_{t+1}) - \mathcal{Q}(s_t, a; \theta_t))\nabla_{\theta_t} \mathcal{Q}(s_t, a; \theta_t)$$

For a given setting where the reward function is not present, the reward function can be estimated from observing trajectories of a functioning policy, i.e. inverse reinforcement learning. The first study that proposed this concept achieves this objective via linear programming (Ng & Russell, 2000).

$$\max \sum_{s \in \mathcal{S}_\rho} \min_{a \in \mathcal{A}} \{\Delta(\mathbb{E}_{s' \sim \mathcal{P}(\cdot|s,a_1)} \mathcal{V}^\pi(s') - \mathbb{E}_{s' \sim \mathcal{P}(\cdot|s,a)} \mathcal{V}^\pi(s'))\}$$

subject to $|\alpha_i| \leq 1$, $i = 1, 2, \ldots, d$, where $\Delta(x) = x$ if $x > 0$ and $\Delta(x) = 2x$ otherwise. While some studies focused on learning the reward function itself others focused on directly learning a policy from demonstrations (Kostrikov et al., 2020). Quite recently, Garg et al. (2021) focused on learning a state-action value function via solely observing the trajectories of a functioning policy (inverse $\mathcal{Q}$-learning), and maximizing the objective function $\mathcal{J}(\theta)$ given by

$$\mathbb{E}_{(s,a)\sim\rho_E}\left[\phi\left(\mathcal{Q}_\theta(s,a) - \gamma \mathbb{E}_{s' \sim \mathcal{P}(\cdot|s,a)}[\mathcal{V}_\theta(s')]\right)\right] - \mathbb{E}_{(s,a)\sim\mu}\left[\phi\left(\mathcal{V}_\theta(s) - \gamma \mathbb{E}_{s' \sim \mathcal{P}(\cdot|s,a)}[\mathcal{V}_\theta(s')]\right)\right]$$

where ρ_E is the occupancy measure of the expert policy, and μ is any valid occupancy measure. The method introduced in this paper achieves state-of-the-art performance in environments with high-dimensional observations. Furthermore, the authors of this study argue that once the state-action value function, i.e. $\mathcal{Q}(s, a)$, is learnt, the reward function, i.e. $r(s_t, a_t, s_{t+1})$, can be reconstructed from this information. Furthermore, note that the inverse $\mathcal{Q}$-learning algorithm can learn a functioning policy and a reward function simultaneously; hence, throughout the paper the inverse $\mathcal{Q}$-learning algorithm will be referred to as an imitation learning and inverse reinforcement learning algorithm interchangeably.

2.2 Robustness and Deep Reinforcement Learning

The adversarial vulnerabilities of deep reinforcement learning policies were initially discussed in Huang et al. (2017). This study essentially introduces fast gradient sign method produced adversarial perturbations (Goodfellow et al., 2015) in to the observation system of the deep reinforcement learning policies. In this line of research some studies tried to further identify adversarial directions (Korkmaz & Brown-Cohen, 2023), while others focused on solving the robustness problem via training with these adversarial directions (Gleave et al., 2020; Pinto et al., 2017). However, recent work demonstrates that the adversarial directions are shared across states, across MDPs and across algorithms (Korkmaz, 2022). Moreover, the certified adversarially trained deep reinforcement learning policies inherit the exact same adversarial directions with the vanilla trained deep reinforcement learning policies. While there are some studies working on the diagnostic perspective of robustness in deep reinforcement learning by using the Carlini & Wagner (2017) formulation, these studies highlight that certified adversarial training shifts vulnerabilities towards a different band in the frequency spectrum instead of eliminating these non-robust features (Korkmaz, 2024). In connection to this, some studies focused on demonstrating the contrast between adversarial and natural directions in terms of their perceptual similarities to the base state observations and the impact they can cause on the policy performance (Korkmaz, 2023). This study demonstrates that the certified adversarial training techniques significantly limit the generalization capabilities of the deep reinforcement learning policies.

3 Foundations for Harmonic Learning

In this section we will introduce harmonic learning (HAL) and provide the foundations and the theoretical analysis for the HAL algorithm. In particular, our algorithm is based on random basis function elimination in a harmonic analytic basis of the state observations during training. Section 4 demonstrates that our theoretically well-founded harmonic learning algorithm results in up to 20$\times$ improvement in sample-efficiency. Section 4.1 and 4.3 will further prove that harmonic learning not only improves the sample complexity but further converges to an intrinsically more robust policy. The theoretical analysis for these results lies in the fact that random harmonic analytic basis elimination can be interpreted as a form of value function randomization, a well-established technique with provable guarantees on sample-efficiency in the function approximation setting. Thus, in order to provide a theoretical foundation for HAL, we connect randomized elimination of basis functions to randomized least-squares value iteration (RLSVI), which provides provable regret bounds via randomization of the learned value function. The setting for the provable regret bounds of RLSVI, including many related follow-up studies (Ladosz et al., 2022; Agarwal et al., 2022), is in finite-horizon, episodic MDPs with linear function approximation of the state-action value function. A finite-horizon MDP with linear function approximation is represented by $M = (\mathcal{S}, \mathcal{A}, \mathcal{P}, r, H)$ where $\mathcal{S}$ is the set of states, and $\mathcal{A}$ the actions. For each $t \in \{1, \dots, H\}$, state s, and action a the transition function $\mathcal{P}_t(\cdot \mid s, a)$ gives the probability distribution over the next state, and the reward function $r_t(s, a)$ outputs the immediate rewards. Let $\Phi_t : \mathcal{S} \times \mathcal{A} \to \mathbb{R}^\kappa$ represent the feature map such that the state-action value function is given by $\mathcal{Q}_{\theta_t}(s, a) = \Phi_t(s, a)^\top \theta_t$. The RLSVI algorithm proceeds in episodes, where in the k-th episode value iteration is performed with a value function that is perturbed by specifically chosen noise η. In particular, for each episode $i \in \{1, \dots, k-1\}$ let (s_{ti}, a_{ti}, r_{ti}) be the state-action-reward tuple observed at time step t. For parameters $\lambda > 0$ and $\sigma > 0$, let $\hat{\theta}_t$ be the parameter estimate for the value function computed via standard least squares value iteration:

$$\hat{\theta}_{t,k} = \arg\min_\theta \left(\frac{1}{\sigma} \sum_{i=1}^{k-1} \left(\Phi_t(s_{ti}, a_{ti})^\top \theta - (r(s_{ti}, a_{ti}) + \max_a \Phi_t(s_{t+1\, i}, a)^\top \theta_{t+1,k} \right)^2 + \lambda \left\| \theta \right\|^2 \right)$$

Then define the regularized regression matrix

$$\Omega_{t,k} = \frac{1}{\sigma^2} \sum_{i=1}^{k-1} \Phi_t(s_{ti}, a_{ti}) \Phi_t(s_{ti}, a_{ti})^\top + \lambda I. \tag{1}$$

The updated parameters of RLSVI are computed by sampling $\eta_{t,k} \sim \mathcal{N}(0, \Omega_{t,k}^{-1})$ and setting $\theta_{t,k} = \hat{\theta}_{t,k} + \eta_{t,k}$. Intuitively, the Gaussian noise $\eta_{t,k}$ added to the value function parameters is chosen to have larger variance along directions where fewer feature vectors $\Phi_t(s_t, a_t)$ have been observed so far, and lower variance along directions with many previously observed feature vectors. This has the effect of directly injecting uncertainty into value estimates proportional to a natural posterior distribution on the parameters. In particular, for any state-action pair $(s_t, a_t) \in \mathcal{S} \times \mathcal{A}$ the state-action value under the random perturbation is given by

$$\mathcal{Q}_{\theta_{t,k}}(s_t, a_t) = \Phi_t(s_t, a_t)^\top (\hat{\theta}_{t,k} + \eta_{t,k}) = \Phi_t(s_t, a_t)^\top \hat{\theta}_{t,k} + \Phi_t(s_t, a_t)^\top \eta_{t,k}$$

$\mathcal{Q}_{\theta_{t,k}}(s_t, a_t) = \mathcal{Q}_{\hat{\theta}_{t,k}}(s_t, a_t) + \Phi_t(s_t, a_t)^\top \eta_{t,k}$. Observe that the value $\Phi_t(s_t, a_t)^\top \eta_{t,k}$ has a Gaussian distribution equal to $\mathcal{N}\left(0, \Phi_t(s_t, a_t)^\top \Omega_{t,k}^{-1} \Phi_t(s_t, a_t)\right)$. Therefore, the random perturbation to each state-action value has variance inversely proportional to a measure of the confidence of the current state-action value estimate. In the general function approximation setting, e.g. when using deep neural networks, it is no longer possible to directly compute the correct noise level to perturb the value estimates via an inversion of the feature covariance matrix. However, we will present an alternative approach, i.e. harmonic learning, that transfers more easily to the general setting, while simultaneously preserving the intuition that the variance should be higher at state-action pairs for which the current $\mathcal{Q}$-function estimate is less confident. To begin we introduce the notion of a stable basis for the feature space of an MDP.

Definition 3.1 (*ϵ-Stable Basis*)**.** Let M be a finite horizon MDP with linear function approximation via feature map $\Phi_t : \mathcal{S} \times \mathcal{A} \to \mathbb{R}^\kappa$ and optimal state-action value function $\mathcal{Q}_{\theta_t^*}$. Let $v_1, \ldots, v_\kappa \in \mathbb{R}^\kappa$ be an orthonormal basis and let $\hat{\Phi}_t(s,a)_i = \Phi(s,a)_t^\top v_i$, The set $v_1, \ldots, v_\kappa$ is an *ϵ-stable basis* for M if for all $s \in \mathcal{S}$, $a \in \mathcal{A}$, and $i \in \{1, \ldots, \kappa\}$

$$\left| \frac{1}{\kappa} \Phi_t(s,a)^\top \theta_t^* - \hat{\Phi}_t(s,a)_i v_i^\top \theta_t^* \right| < \epsilon$$

To gain an intuition for Definition 3.1, observe that for any orthonormal basis $v_1, \ldots, v_\kappa$ the feature vector can be written as the linear combination $\sum_i \hat{\Phi}_t(s,a)_i v_i$. Thus, the definition requires that each component $\hat{\Phi}_t(s,a)_i v_i$ of the feature vector along direction v_i contributes approximately a $\frac{1}{\kappa}$ fraction of the optimal state action value $\mathcal{Q}_{\theta_t^*}(s,a) = \Phi_t(s,a)^\top \theta_t^*$. This property is analogous to the uncertainty principle in harmonic analysis, which qualitatively states that signals which are localized with respect to the standard basis must be more evenly spread out with respect to the harmonic analytic basis. Given a stable basis, there is a natural measure of uncertainty for any estimate of the state-action value function.

Definition 3.2 (*Uncertainty of Parameters*)**.** Let $v_1, \ldots, v_\kappa$ be an ϵ-stable basis for M. For any parameter estimate θ_t for the state-action values the *uncertainty* of θ_t for action a in state s is

$$\Upsilon_{\theta_t}(s,a) = \frac{1}{\kappa} \sum_i \left(\frac{1}{\kappa} \Phi_t(s,a)^\top \theta_t - \hat{\Phi}_t(s,a)_i v_i^\top \theta_t \right)^2.$$

Observe that for the optimal parameters θ^* we have $\Upsilon_{\theta_t^*}(s,a) < \epsilon^2$. In general, the uncertainty measures how far the estimate θ_t deviates from having an equal contribution from the components of the feature map $\Phi_t(s,a)$ along each of the basis vectors v_i. Since the vectors v_i form a stable-basis (and thus the contribution in each component to the optimal state-action value should be equal), larger values for the uncertainty implies that the estimate θ_t is further from the optimum for action a in state s. We now have all the ingredients to introduce the foundations for harmonic learning. Essentially, Algorithm 1 adds noise to the value function by removing the component of the feature $\Phi_t(s,a)$ along a randomly chosen stable-basis direction v_i.

Algorithm 1 Stable-basis noise

1: **Input:** A stable basis $v_1, \ldots, v_\kappa$ for an MDP M. An estimate θ_t for the state-action value function, a state s, and action a.
2: Sample i uniformly at random from $\{1, \ldots, \kappa\}$
3: Set $\tilde{\Phi}_t(s,a) = \Phi_t(s,a) - \hat{\Phi}_t(s,a)_i v_i$
4: Output the noisy state-action value $\tilde{\Phi}_t(s,a)^\top \theta_t$

Proposition 3.3 (*Stable-basis noise variance*)**.** *Let $v_1, \dots, v_\kappa$ be an ϵ-stable basis for M. For parameter vector θ_t, let $\tilde{\mathcal{Q}}_{\theta_t}(s,a)$ be the state-action value estimate output by Algorithm 1. Let $\eta = \tilde{\mathcal{Q}}_{\theta_t}(s,a) - \mathcal{Q}_{\theta_t}(s,a)$. Then* $\mathrm{Var}[\eta] = \Upsilon_{\theta_t}(s,a)$.

Proof. First observe that $\mathbb{E}[\eta] = \mathbb{E}[\tilde{\mathcal{Q}}_{\theta_t}(s,a) - \mathcal{Q}_{\theta_t}(s,a)]$, and

$$\mathbb{E}[\eta] = \mathbb{E}_i \left[(\Phi_t(s,a) - \hat{\Phi}_t(s,a)_i v_i)^\top \theta_t - \Phi_t(s,a)^\top \theta_t \right] = -\mathbb{E}_i \left[\hat{\Phi}_t(s,a)_i v_i^\top \theta_t \right] = -\frac{1}{\kappa} \Phi_t(s,a)^\top \theta_t$$

Therefore, the variance of the noise η is given by

$$\begin{aligned} \mathrm{Var}[\eta] &= \mathbb{E} \left[\left(\tilde{\mathcal{Q}}_{\theta_t}(s,a) - \mathcal{Q}_{\theta_t}(s,a) + \frac{1}{\kappa} \Phi_t(s,a)^\top \theta_t \right)^2 \right] \\ &= \mathbb{E}_i \left[\left(\frac{1}{\kappa} \Phi_t(s,a)^\top \theta_t - \hat{\Phi}_t(s,a)_i v_i^\top \theta_t \right)^2 \right] = \Upsilon_{\theta_t}(s,a) \end{aligned}$$ □

Random modification of the value function via Algorithm 1 is equivalent to adding noise η to $\mathcal{Q}_{\theta_t}(s,a)$ where the variance of the noise η is exactly equal to the uncertainty $\Upsilon_{\theta_t}(s,a)$. Thus, by simply deleting the component of the feature vector along a randomly selected stable-basis vector, one can add noise that has variance proportional to a natural uncertainty measure for the current parameter estimate.

3.1 General Function Approximation

It is now straightforward to extend both the definition of a stable basis and Algorithm 1 to the general function approximation setting. In this setting we will assume that the state space $\mathcal{S}$ is a d-dimensional vector space, the action space $\mathcal{A}$ is finite, and the optimal state-action value function $\mathcal{Q}^*(s,a)$ is a general function on $\mathcal{S} \times \mathcal{A}$.

Definition 3.4 (*General Function Approximation*)**.** Let M be an MDP and $\epsilon > 0$. An ϵ-stable basis for M is an orthonormal basis $v_1, \dots, v_\kappa$ for $\mathcal{S}$ such that for all i,

$$\left| \mathcal{Q}^*(s,a) - \mathcal{Q}^*(s - (v_i^\top s) v_i, a) \right| < \frac{1}{\kappa} \mathcal{Q}^*(s,a) + \epsilon.$$

Algorithm 1 can also be easily modified for the general function approximation setting by sampling a random i, and replacing the state s with $\tilde{s} = s - (v_i^\top s) v_i$ i.e. by sampling a random i and deleting the component of s along v_i. The following proposition shows that in the general function approximation setting, one can test for the presence of a stable basis by modifying states via Algorithm 1 and measuring cumulative rewards.

Proposition 3.5. *Let $v_1, \dots, v_\kappa$ be an ϵ-stable basis for an MDP M. For a state s let $a^*(s) = \arg\max_a \mathcal{Q}^*(s,a)$ be the argmax action. Assume that $\epsilon < \frac{1}{2} \left(\frac{\kappa-1}{\kappa} \mathcal{Q}^*(s, a^*(s)) - \arg\max_{a \neq a^*(s)} \frac{\kappa+1}{\kappa} \mathcal{Q}^*(s,a) \right)$ for all $s \in S$. Let R^* be the expected cumulative rewards when following the argmax policy according to $\mathcal{Q}^*$. Then if each state is modified according to the general function approximation version of Algorithm 1 the expected cumulative discounted rewards R obtained under the argmax policy satisfies $R = R^*$.*

Proof. Under the general function approximation version of Algorithm 1 each state s encountered is modified to $\tilde{s} = s - (v_i^\top s v_i)$. By Definition 3.4 for the action $a^*(s)$

$$\mathcal{Q}^*(\tilde{s}, a^*(s)) > \mathcal{Q}^*(s, a^*(s)) - \frac{1}{\kappa} \mathcal{Q}^*(s, a^*(s)) - \epsilon = \frac{\kappa - 1}{\kappa} \mathcal{Q}^*(s, a^*(s)) - \epsilon \tag{2}$$

Similarly, by Definition 3.4, for any $a \neq \arg\max_a \mathcal{Q}(s,a)$

$$\mathcal{Q}^*(\tilde{s}, a) < \frac{\kappa + 1}{\kappa} \mathcal{Q}^*(s,a) + \epsilon \leq \arg\max_{a \neq a^*(s)} \frac{\kappa + 1}{\kappa} \mathcal{Q}^*(s,a) + \epsilon. \tag{3}$$

Combining (2) and (3) with the assumption on ϵ implies that $\mathcal{Q}^*(\tilde{s}, a) < \mathcal{Q}^*(\tilde{s}, a^*(s))$ for all $a \neq a^*(s)$. Thus the argmax action in each state under Algorithm 1 is equal to the argmax action in the original unmodified state, implying that the distribution of the trajectory and the cumulative rewards remain unchanged. □

Algorithm 2 HAL: Harmonic Learning

Input: Occupancy measure of the expert policy ρ_E, regularizer ϕ, κ dimension of the state observations, μ experiences from replay buffer, learning rate $\alpha_{\mathcal{Q}}$, actions $a \in \mathcal{A}$, states $s \in \mathcal{S}$, initialize $\mathcal{Q}_{\theta_0}$ and stable basis frequency Ψ.
for $t = 0$ **to** N **do**
  for $s = s_0$ **to** s_T **do**
    Sample $\delta \sim \mathcal{U}(0, \kappa/2)$
    $\mathcal{F}_s(u,v) = \frac{1}{\kappa^2} \sum_{m=0}^{\kappa-1} \sum_{n=0}^{\kappa-1} s(m,n) e^{-j2\pi((um+vn)/d)}$
    $\mathcal{F}_s[\delta, \delta : \kappa - \delta] = \mathcal{F}_s[\kappa - \delta, \delta : \kappa - \delta] = \mathcal{F}_s[\delta : \kappa - \delta, \delta] = \mathcal{F}_s[\delta : \kappa - \delta, \kappa - \delta] = \Psi$
    $s^{\text{spc}}(m,n) = \sum_{u=0}^{\kappa-1} \sum_{v=0}^{\kappa-1} \mathcal{F}(u,v) e^{j2\pi((um+vn)/\kappa)}$
    Insert s^{spc} to the buffer instead of s
    Train $\mathcal{Q}$ function:
    $\tilde{\mathcal{V}}(s) = \mathbb{E}_{(s,a)\sim\mu}[\mathcal{V}_{\theta_t}(s)] - \gamma \mathbb{E}_{s' \sim \mathcal{P}(\cdot|s,a)}[\mathcal{V}_{\theta_t}(s')]$
    $\mathcal{Z} = \nabla_{\theta_t}[\mathbb{E}_{\rho_E} \phi(\mathcal{Q}_{\theta_t}(s,a) - \gamma \mathbb{E}_{s' \sim \mathcal{P}(\cdot|s,a)} \mathcal{V}_{\theta_t}(s'))]$
    $\theta_{t+1} \leftarrow \theta_t + \alpha_{\mathcal{Q}} \mathcal{Z} - \alpha_{\mathcal{Q}} \nabla_{\theta_t} \tilde{\mathcal{V}}(s)$
  end for
end for
Return: State-action value function $\mathcal{Q}_{\theta_N}(s,a)$

The Fourier basis is one of the natural choices for a stable basis. Naturally occurring observations in the real world are highly non-sparse in the Fourier basis, and thus removing the component along any Fourier basis vector is unlikely to cause a semantically meaningful change within the observation. Thus, the optimal robust policy when learning from high-dimensional observations should not have particularly large dependence on any one part of the Fourier basis corresponding to a particular frequency. The empirical results of Section 4 further provides evidence that the Fourier basis forms a stable basis for deep reinforcement learning policies trained with high-dimensional state-observations. In particular Figure 5 demonstrates that removing each subset of elements of the basis corresponding to one particular frequency has approximately equal impact on vanilla trained policy performance. On the other hand inverse-$\mathcal{Q}$ learning, which uses fewer environment interactions, has much larger variation in policy sensitivity across frequencies. Thus, the policy that is trained with more interactions, and thus is closer to optimal, satisfies the conditions of Definition 3.1 with respect to the Fourier basis. Therefore, we can extend our method from Algorithm 1 to learning from high-dimensional state observations by leveraging randomized removal of the elements of the stable basis, i.e. removing components of the state-observation in the Fourier basis in order to induce uncertainty in the value function to boost sample-efficiency.

4 Harmonic Learning in High Dimensional MDPs

While Section 3 provides theoretical justification for our proposed training method in this section we provide details into the harmonic learning algorithm. In particular, Algorithm 2 provides pseudocode for the harmonic learning method. Note that visualizations of transformations of the elements of the stable basis of state observations are also demonstrated in Figure 3. The experiments provided in our paper are conducted in the Arcade Learning Environment (Bellemare et al., 2013). All of the MDPs considered in our paper have high-dimensional state representations. The deep reinforcement learning policies used in stable basis robustness analysis are trained via double-$\mathcal{Q}$ learning (van Hasselt et al., 2016; van Hasselt, 2010). Natural robustness was measured with the same parameters used in (Korkmaz, 2024). The experiments are conducted with 10 random runs. The standard error of the mean is included in all of the results presented throughout the paper. All of the policies that are trained without the reward signal from the MDP uses the exact same hyperparameters with inverse $\mathcal{Q}$-learning algorithm (Section 2.1) to provide consistent and transparent comparison where the batch size 32, the network consists of 2 hidden layers with 64 units. See supplementary material for the code, the hyperparameters and architecture details.

Table 1 reports the raw scores and human normalized scores for the inverse $\mathcal{Q}$-learning algorithm and the harmonic learning algorithm in Pong, Breakout, Seaquest, SpaceInvaders and BeamRider. As Table 1 reports, the performance obtained by the harmonic learning over inverse $\mathcal{Q}$-learning in

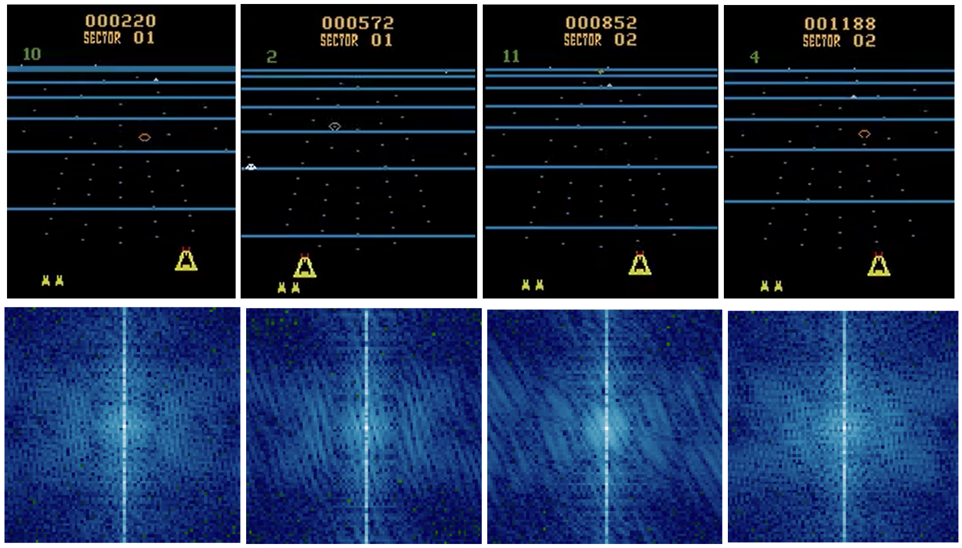

Figure 1: State observations of the high-dimensional state representation MDPs and the spectral properties and representations in BeamRider.

Table 1: Performance analysis results for harmonic learning and inverse $\mathcal{Q}$-learning in Pong, Breakout, Seaquest, SpaceInvaders and BeamRider. Table reports raw scores and human normalized scores for harmonic learning and inverse $\mathcal{Q}$-learning.

Performance Analysis	Raw Scores		Human Normalized Scores	
Training Method	Harmonic Learning	Inverse $\mathcal{Q}$-learning	Harmonic Learning	Inverse $\mathcal{Q}$-learning
Pong	**19.0±1.89736**	8.0±5.3814	**1.3233± 0.0199**	0.9566±0.05672
Seaquest	**906.0±53.2202**	864.0±42.0285	**0.04164±0.00083**	0.03955±0.00066
SpaceInvader	**609.0±14.5223**	470.555±23.6812	**0.3064±0.003052**	0.2144±0.00497
BeamRider	**1023.6±140.974**	909.6±65.392	**0.1219±0.0082**	0.1008±0.0038
Breakout	**228.8± 35.4606**	108.9±29.7198	**7.5448±0.37254**	3.5614±0.3122

Breakout is 210%. Furthermore, intriguingly the harmonic learning algorithm can reach a score of 19.0 for Pong in **only 50K environment interactions**, where inverse-$\mathcal{Q}$ learning is unable to reach this score even with 1 million environment interactions after convergence. Thus, harmonic learning is not only sample-efficient but further simply converges to a substantially better policy as an end product. Figure 5 reports robustness analysis results for harmonic learning and inverse $\mathcal{Q}$-learning. Intriguingly, these results demonstrate that the inverse $\mathcal{Q}$-learning policies result in high-frequency oscillations compared to deep neural policies trained via harmonic learning. The fact that deep neural policies trained via harmonic learning obtain dampened oscillations on the robustness analysis, i.e. an analysis that measures robustness via direct policy performance, demonstrates that harmonic learning, on top of the sample efficiency it gains as demonstrated in Table 1, further learns more robust and resilient policies.

4.1 Stable Basis Robustness Analysis of Deep Sequential Decision Making

While Section 3 provides the foundations and the theoretical analysis for harmonic learning, Section 4 provides the empirical analysis of the harmonic learning algorithm in high-dimensional complex MDPs. These results demonstrate that harmonic learning improves sample efficiency by up to $20\times$. Yet, our objective was not only to improve sample complexity but further to construct policies that can make robust and resilient decisions in uncertain non-stationary environments. In this section we will introduce the techniques that quantify the volatilities in decision making. In particular, the objective of Stable Basis Robustness Analysis (SBRA) is to quantify and measure the impact of the elements of the stable basis on the policy performance. The stable basis in this analysis was set to the Fourier basis, yet it is further possible to establish a different type of basis as stable, as long as the basis satisfies $\left|\frac{1}{\kappa}\Phi_t(s,a)^\top\theta_t^* - \hat{\Phi}_t(s,a)_i v_i^\top\theta_t^*\right| < \epsilon$. Upon the setting the δ-frequencies to Ψ the discrete Fourier transform is inverted and the observation of the deep neural policy consists of s^{spc} as in Algorithm 3. Figure 3 provides the steps of the stable basis robustness analysis (SBRA) with variations of δ. For a state $s \in \mathcal{S}$ the discrete Fourier transform of the state s is

$$\mathcal{F}_s(u,v) = \frac{1}{\mathcal{M}\mathcal{N}} \sum_{m=0}^{\mathcal{M}-1} \sum_{n=0}^{\mathcal{N}-1} s(m,n) e^{-j2\pi(um/\mathcal{M} + vn/\mathcal{N})}$$

The impact on the policy performance is measured by $\mathcal{I} = (\text{Score}_{\text{baseline}} - \text{Score}_{\mathcal{F}_s})/(\text{Score}_{\text{baseline}})$, where $\text{Score}_{\mathcal{F}_s}$ represents the score obtained by the deep neural policy when the state observations are transformed as described in Algorithm 3, and $\text{Score}_{\text{baseline}}$ represents the score obtained by the baseline policy without any modifications applied to the state observations. Figure 2 reports results on the stable basis robustness analysis of the deep reinforcement learning policy and the deep inverse reinforcement learning policy as the randomized δ-frequencies are transformed to Ψ. The results reported in Figure 2 demonstrate that vanilla trained deep reinforcement learning policies are more robust than the policies trained via deep inverse reinforcement learning. In particular, there is a high increase in the sensitivities towards lower frequencies for the deep inverse reinforcement learning policy.

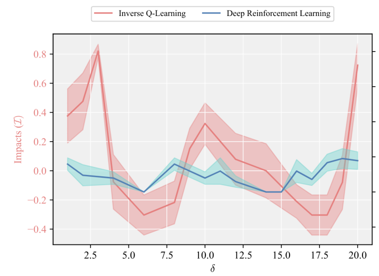

Figure 2: Stable Basis Robustness Analysis (SBRA) results for the deep reinforcement learning policy and the state-of-the-art deep inverse reinforcement learning policy.

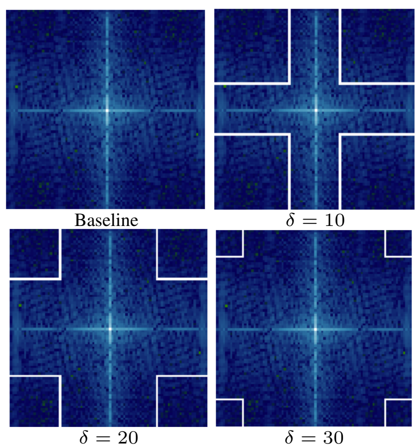

Figure 3: Stable Basis Robustness Analysis (SBRA) with variations of δ .

Algorithm 3 SBRA: Stable Basis Robustness Analysis

Input: State-action value function $\mathcal{Q}(s,a)$, actions $a \in \mathcal{A}$, states $s \in \mathcal{S}$, stable basis robustness analysis frequency Ψ, policy $\pi(s,a)$, κ dimension of the state observations
Output: Impact on the policy performance
for $\delta = 0$ **to** $\kappa/2$ **do**
  for $s = s_0$ **to** s_T **do**
    $\mathcal{F}_s(u,v) = \frac{1}{\kappa^2} \sum_{m=0}^{\kappa-1} \sum_{n=0}^{\kappa-1} s(m,n) e^{-j2\pi((um+vn)/\kappa)}$
    $\mathcal{F}_s[\delta, \delta : \kappa - \delta] = \mathcal{F}_s[\kappa - \delta, \delta : \kappa - \delta] = \Psi$
    $\mathcal{F}_s[\delta : \kappa - \delta, \delta] = \mathcal{F}_s[\delta : \kappa - \delta, \kappa - \delta] = \Psi$
    $s^{\text{spc}}(m,n) = \sum_{u=0}^{\kappa-1} \sum_{v=0}^{\kappa-1} \mathcal{F}(u,v) e^{j2\pi((um+vn)/\kappa)}$
    $\hat{a}(s) = \arg\max_{a \in \mathcal{A}} \mathcal{Q}(s^{\text{spc}}, a)$
  end for
end for
Return: Impact $\mathcal{I}$

4.2 Overfitting of State-Action Value Function in Inverse Reinforcement Learning

The results reported in this section demonstrate that inverse $\mathcal{Q}$-learning assigns higher state-action values than harmonic learning, even though the rewards obtained are lower compared to harmonic learning. In particular, Figure 4 reports the state-action value of the action maximizing the state-action value function in a given state for deep neural policies trained via harmonic learning and inverse $\mathcal{Q}$-learning policies. Table 2 reports the average total rewards obtained and the average state-action values of the actions that maximize the state-action value function in a given state

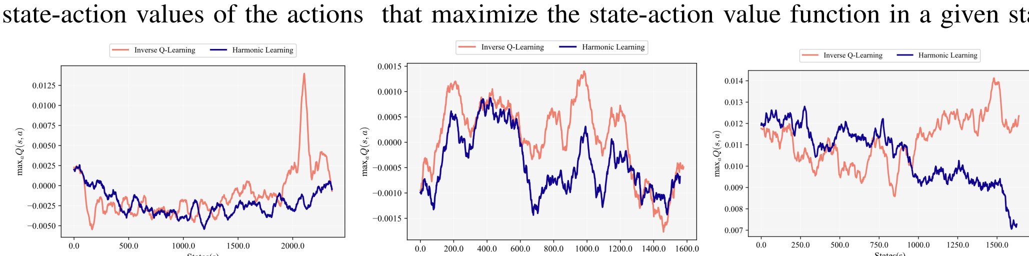

Figure 4: State-action values for the deep neural policies trained via harmonic learning and inverse $\mathcal{Q}$-learning policies. Left: BeamRider. Center: Pong. Right: Breakout.

Table 2: Average rewards obtained and average state-action values of the actions maximizing the state-action value function in a given state (i.e. $\mathbb{E}_{s\sim e(s),e\sim\varepsilon(e)}[\max_a \mathcal{Q}(s,a)]$) for harmonic learning and inverse $\mathcal{Q}$-learning policies in Pong, Breakout, SpaceInvaders and BeamRider.

$\mathcal{Q}$ Analysis	$\mathbb{E}_{s\sim e(s),e\sim\varepsilon(e)}[\max_a \mathcal{Q}(s,a)]$		Average Rewards	
Method	Harmonic Learning	Inverse $\mathcal{Q}$-learning	Harmonic Learning	Inverse $\mathcal{Q}$-learning
SpaceInvader	**0.001291±0.0001532**	-0.000188±7.55×10^{-5}	**602.0±13.023056**	528.5±18.9347
BeamRider	**-0.001739±4.34×10^{-5}**	-0.001808±2.17×10^{-5}	**1108.4± 158.10725**	908.8±95.039865
Breakout	0.009761±6.25×10^{-5}	**0.01085±3.70×10^{-5}**	**214.3±38.5888**	39.0±6.1967
Pong	-0.0007503±3.67×10^{-5}	**-0.000455±7.60×10^{-5}**	**19.0±1.89736**	8.0±5.3814

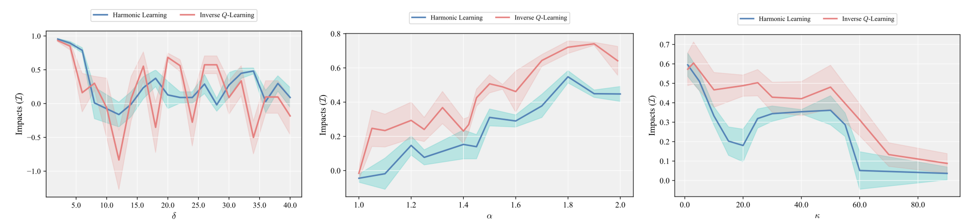

SBRA Contrast DCT Artifacts

Figure 5: Left: Robustness analysis with SBRA for harmonic learning and inverse $\mathcal{Q}$-learning policies in Breakout. Center: The impact results for natural robustness analysis with non-robust directions intrinsic to the MDP for contrast in SpaceInvaders. Right: The impact results of natural perturbations intrinsic to the MDP for discrete cosine transform artifacts in SpaceInvaders.

(i.e. $\mathbb{E}_{s\sim e(s),e\sim\varepsilon(e)}[\max_a \mathcal{Q}(s,a)]$) for harmonic learning and inverse $\mathcal{Q}$-learning policies. The fact that inverse $\mathcal{Q}$-learning policies construct a state-action value function that assigns higher values while the true rewards obtained are lower demonstrates that inverse $\mathcal{Q}$-learning results in learning overestimated state-action values. Hence, harmonic learning further targets the overfitting problem of the state-action value function and results in lowering the overestimation bias in state-action values compared to the baseline training methods.

4.3 Natural Robustness and Generalization

In this section we provide a detailed analysis on the robustness of deep sequential decision making policies to distributional shift. In particular, recent work connected the relationship between adversarial robustness and natural robustness in a given MDP in terms of the damage caused by these natural directions in the deep neural policy landscape on the policy performance and the perceptual similarity distances to the base state observations. In particular, the imperceptibility $\mathcal{P}_{\text{similarity}}$ is measured by, $\mathcal{P}_{\text{similarity}}(s, s+\xi(s,\pi)) = \sum_l \frac{1}{H_l W_l} \sum_{h,w} \| w_l \odot (\hat{y}^l_{shw} - \hat{y}^l_{(s+\xi(s,\pi))hw}) \|_2^2$ where $\hat{y}^l_s, \hat{y}^l_{\hat{s}} \in \mathbb{R}^{W_l \times H_l \times C_l}$ represent the vector of activations in the convolutional layers with width W_l, height H_l, C_l is the number of channels, and $\xi(s,\pi)$ natural change function[1]. Note that Section 4.1 demonstrates in detail that policies that learn from observing an expert without having access to the reward function are less robust compared to deep reinforcement learning policies. In many prominent settings, e.g. large language models as in RLHF and self driving cars, constructing a reward function is substantially more difficult than learning one from demonstrations, and achieving more sample efficient and robust policies carries significant importance given both the safety and security concerns that have been recently raised (Washington Post, 2023; New York Times, November 2023). Hence, in this section we provide a comprehensive investigation on the robustness and Figure 5 reports the performance profile results under these natural directions for harmonic learning and inverse $\mathcal{Q}$-learning policies. In particular, the results reported in Figure 5 demonstrate that harmonic learning results in intrinsically more robust deep neural policies that can generalize to observations that have not been seen before by the policy (i.e. points that are outside of the training environment). These results once more demonstrate that harmonic learning not only results in learning sample-efficient policies but also further learns policies that are both robust and generalizable.

[1]In connection with the contradistinction between adversarial and natural robustness, recently it has been shown that standard reinforcement learning policies are more robust and can generalize better compared to certified robust (i.e. adversarial) trained ones by the natural robustness framework (Korkmaz, 2023).

5 CONCLUSION

In this paper we aim to seek answers for the following questions: *(i) How can we make deep sequential decision making policies that can learn from high-dimensional state observations more robust and more sample efficient? (ii) What are the fundamental differences between learning via exploration vs learning via observing experts that limit policies to robustly generalize to uncertain environments?*, *(iii) Is it possible to simultaneously improve sample efficiency without sacrificing robustness?* To be able to address these questions we propose a theoretically well-founded training algorithm that leverages the spectral perspective in deep sequential decision making. We conduct extensive experiments in the Arcade Learning Environment and the empirical analysis demonstrates that our proposed algorithm results in exceptional sample efficiency improvement. Moreover, we propose a novel method that provides a comprehensive analysis of the robustness and instabilities of deep neural policies. We provide further extensive investigation on the state-action value function learned by the deep neural policies and demonstrate that prior methods suffer from overestimation problems. Furthermore, we conduct a robustness analysis that investigates the response of the deep sequential decision making policies to distributional shift. The results provided in our paper demonstrate that the theoretically well-founded harmonic learning algorithm we introduce results in exceptionally sample-efficient, and furthermore substantially robust and resilient deep neural policies.

REFERENCES

David Abel, Andre Barreto, Benjamin Van Roy, Doina Precup, Hado van Hasselt, and Satinder Singh. A definition of continual reinforcement learning. In *Thirty-seventh Annual Conference on Neural Information Processing Systems, NeurIPs 2023*, 2023.

Alekh Agarwal, Nan Jiang, Sham M. Kakade, and Wen Sun. Reinforcement learning: Theory and algorithms. 2022.

Marc G Bellemare, Yavar Naddaf, Joel Veness, and Michael. Bowling. The arcade learning environment: An evaluation platform for general agents. *Journal of Artificial Intelligence Research.*, pp. 253–279, 2013.

Nicholas Carlini and David Wagner. Towards evaluating the robustness of neural networks. *In 2017 IEEE Symposium on Security and Privacy (SP)*, pp. 39–57, 2017.

Kenji Doya and Terrence Sejnowski. A novel reinforcement model of birdsong vocalization learning. *Conference on Neural Information Processing Systems (NeurIPS)*, 1994.

Alhussein Fawzi, Matej Balog, Aja Huang, Thomas Hubert, Bernardino Romera-Paredes, Mohammadamin Barekatain, Alexander Novikov, Francisco J. R. Ruiz, Julian Schrittwieser, Grzegorz Swirszcz, David Silver, Demis Hassabis, and Pushmeet Kohli. Discovering faster matrix multiplication algorithms with reinforcement learning. *Nature*, 610(7930):47–53, 2022.

Sebastian Flennerhag, Tom Zahavy, Brendan O'Donoghue, Hado van Hasselt, András György, and Satinder Singh. Optimistic meta-gradients. In *Thirty-seventh Annual Conference on Neural Information Processing Systems, NeurIPs 2023*, 2023.

Divyansh Garg, Shuvam Chakraborty, Chris Cundy, Jiaming Song, and Stefano Ermon. Iq-learn: Inverse soft-q learning for imitation. *Neural Information Processing Systems (NeurIPS) [Spotlight Presentation]*, 2021.

Adam Gleave, Michael Dennis, Cody Wild, Kant Neel, Sergey Levine, and Stuart Russell. Adversarial policies: Attacking deep reinforcement learning. *International Conference on Learning Representations ICLR*, 2020.

Ian Goodfellow, Jonathan Shelens, and Christian Szegedy. Explaning and harnessing adversarial examples. *International Conference on Learning Representations*, 2015.

Sandy Huang, Nicholas Papernot, Yan Goodfellow, Ian an Duan, and Pieter Abbeel. Adversarial attacks on neural network policies. *Workshop Track of the 5th International Conference on Learning Representations*, 2017.

Sham Machandranath Kakade. On the sample complexity of reinforcement learning. *Nature*, 2003.

Steven Kapturowski, Victor Campos, Ray Jiang, Nemanja Rakicevic, Hado van Hasselt, Charles Blundell, and Adrià Puigdomènech Badia. Human-level atari 200x faster. In *The Eleventh International Conference on Learning Representations, ICLR 2023*, 2023.

Michael Kearns and Satinder Singh. Finite sample convergence rates for q-learning and indirect algorithms. *Conference on Neural Information Processing Systems (NeurIPS)*, 1999.

Ezgi Korkmaz. Deep reinforcement learning policies learn shared adversarial features across MDPs. *Proceedings of the AAAI Conference on Artificial Intelligence*, pp. 7229–7238, 2022.

Ezgi Korkmaz. Adversarial robust deep reinforcement learning requires redefining robustness. In *Thirty-Seventh AAAI Conference on Artificial Intelligence, AAAI 2023, Washington, DC, USA, February 7-14, 2023*, pp. 8369–8377. AAAI Press, 2023.

Ezgi Korkmaz. Diagnosing and understanding deep reinforcement learning decision making. In *Proceedings of the 41th International Conference on Machine Learning*, Proceedings of Machine Learning Research. PMLR, 2024.

Ezgi Korkmaz and Jonah Brown-Cohen. Detecting adversarial directions in deep reinforcement learning to make robust decisions. In *Proceedings of the 40th International Conference on Machine Learning*, volume 202 of *Proceedings of Machine Learning Research*, pp. 17534–17543. PMLR, 23–29 Jul 2023.

Maria Korshunova, Niles Huang, Stephen Capuzzi, Dmytro S. Radchenko, Olena Savych, Yuriy S. Moroz, Carrow I. Wells, Timothy M. Willson, Alexander Tropsha, and Olexandr Isayev. Generative and reinforcement learning approaches for the automated de novo design of bioactive compounds. *Nature Chemistry*, 2022.

Ilya Kostrikov, Ofir Nachum, and Jonathan Tompson. Imitation learning via off-policy distribution matching. In *8th International Conference on Learning Representations, ICLR 2020, Addis Ababa, Ethiopia, April 26-30, 2020*, 2020.

Pawel Ladosz, Lilian Weng, Minwoo Kim, and Hyondong Oh. Exploration in deep reinforcement learning: A survey. *https://arxiv.org/pdf/2205.00824*, 2022.

Daniel J. Mankowitz, Andrea Michi, Anton Zhernov, Marco Gelmi, Marco Selvi, Cosmin Paduraru, Edouard Leurent, Shariq Iqbal, Jean-Baptiste Lespiau, Alex Ahern, Thomas Köppe, Kevin Millikin, Stephen Gaffney, Sophie Elster, Jackson Broshear, Chris Gamble, Kieran Milan, Robert Tung, Minjae Hwang, Taylan Cemgil, Mohammadamin Barekatain, Yujia Li, Amol Mandhane, Thomas Hubert, Julian Schrittwieser, Demis Hassabis, Pushmeet Kohli, Martin A. Riedmiller, Oriol Vinyals, and David Silver. Faster sorting algorithms discovered using deep reinforcement learning. *Nature*, 618(7964):257–263, 2023.

Volodymyr Mnih, Adria Badia Puigdomenech, Mehdi Mirza, Alex Graves, Timothy Lillicrap, Tim Harley, David Silver, and Koray. Kavukcuoglu. Asynchronous methods for deep reinforcement learning. *In International Conference on Machine Learning*, pp. 1928–1937, 2016.

P. Read Montague, Peter Dayan, Christophe Person, and Terrence J. Sejnowski. Bee foraging in uncertain environments using predictive hebbian learning. *Nature*, 377:725–728, 1995.

New York Times. Global leaders warn a.i. could cause 'catastrophic' harm. November 2023.

Andrew Y. Ng and Stuart J. Russell. Algorithms for inverse reinforcement learning. In Pat Langley (ed.), *Proceedings of the Seventeenth International Conference on Machine Learning (ICML 2000), Stanford University, Stanford, CA, USA, June 29 - July 2, 2000*, pp. 663–670, 2000.

Lerrel Pinto, James Davidson, Rahul Sukthankar, and Abhinav Gupta. Robust adversarial reinforcement learning. *International Conference on Learning Representations ICLR*, 2017.

Mariya Popova, Olexandr Isayev, and Alexander. Tropsha. Deep reinforcement learning for de novo drug design. *Science advances 4*, 78, 2018.

Nestor A. Schmajuk and B. Silvano Zanutto. Escape, avoidance, and imitation: A neural network approach. *Adaptive Behaviour*, 1997.

Julian Schrittwieser, Ioannis Antonoglou, Thomas Hubert, Karen Simonyan, Laurent Sifre, Simon Schmitt, Arthur Guez, Edward Lockhart, Demis Hassabis, Thore Graepel, Timothy P. Lillicrap, and David Silver. Mastering atari, go, chess and shogi by planning with a learned model. *Nature*, 588, 2020.

Hugo Touvron, Thibaut Lavril, Gautier Izacard, Xavier Martinet, Marie-Anne Lachaux, Timothée Lacroix, Baptiste Rozière, Naman Goyal, Eric Hambro, Faisal Azhar, Aurélien Rodriguez, Armand Joulin, Edouard Grave, and Guillaume Lample. Llama: Open and efficient foundation language models. *CoRR*, abs/2302.13971, 2023.

Hado van Hasselt. Double q-learning. In John D. Lafferty, Christopher K. I. Williams, John Shawe-Taylor, Richard S. Zemel, and Aron Culotta (eds.), *Advances in Neural Information Processing Systems 23: 24th Annual Conference on Neural Information Processing Systems 2010. Proceedings of a meeting held 6-9 December 2010, Vancouver, British Columbia, Canada*, pp. 2613–2621. Curran Associates, Inc., 2010.

Hado van Hasselt, Arthur Guez, and David Silver. Deep reinforcement learning with double q-learning. In *Proceedings of the Thirtieth AAAI Conference on Artificial Intelligence, February 12-17, 2016, Phoenix, Arizona, USA*, pp. 2094–2100. AAAI Press, 2016.

The Washington Post. 17 fatalities, 736 crashes: The shocking toll of tesla's autopilot. 2023.

Chris Watkins. Learning from delayed rewards. In *PhD thesis, Cambridge*. King's College, 1989.